



# The Open Materials Science Journal

Content list available at: [www.benthamopen.com/TOMSJ/](http://www.benthamopen.com/TOMSJ/)

DOI: 10.2174/1874088X01812010029



## RESEARCH ARTICLE

# Process Optimization for the Synthesis of Silver (AgNPs), Iron Oxide ( $\alpha$ -Fe<sub>2</sub>O<sub>3</sub>NPs) and Core-Shell (Ag-Fe<sub>2</sub>O<sub>3</sub>CNPs) Nanoparticles Using the Aqueous Extract of *Alstonia Scholaris*: A Greener Approach

Navinchandra G. Shimpi<sup>1,\*</sup>, Mujahid Khan<sup>1</sup>, Sharda Shirole<sup>2</sup> and Shriram Sonawane<sup>3</sup><sup>1</sup>Department of Chemistry, University of Mumbai, Sant Cruz (E) 400 098, India<sup>2</sup>University Institute of Chemical Technology, North Maharashtra University, Jalgaon, India<sup>3</sup>Department of Chemical Engineering Visvesvaraya National Institute of Technology, Nagpur

Received: February 12, 2018

Revised: March 31, 2018

Accepted: May 21, 2018

### Abstract:

#### Objective:

The present study deals with the green synthesis of silver (AgNPs), iron oxide ( $\alpha$ -Fe<sub>2</sub>O<sub>3</sub>NPs) and core-shell (Ag- $\alpha$ -Fe<sub>2</sub>O<sub>3</sub>CNPs) nanoparticles using the aqueous extract of *Alstonia scholaris* without any catalyst, template or surfactant or any intermediate under ultrasound cavitation technique. The purpose was to facilitate the high level of dispersion with increase in rate of reaction. Further AgNPs and  $\alpha$ -Fe<sub>2</sub>O<sub>3</sub>NPs were used to synthesize Ag-Fe<sub>2</sub>O<sub>3</sub>CNPs in aqueous extract of *Alstonia scholaris* under controlled ultrasound cavitation technique.

#### Methods:

The size of AgNPs and Ag-Fe<sub>2</sub>O<sub>3</sub>CNPs can be tuned by optimizing various reaction parameters. UV-visible, X-ray diffraction spectroscopy (XRD), Transmission electron microscopy (TEM), Field emission scanning electron microscope (FE-SEM) and Fourier transform infra-red spectroscopy has been used for the characterization of silver and core shell Ag@Fe<sub>2</sub>O<sub>3</sub> nanoparticles. TEM images clearly show the formation of core shell nanoparticles with spherical morphology.

#### Result:

Fourier transform infra-red spectroscopy analysis revealed that carbohydrate, polyphenols, and protein molecules were involved in the synthesis and capping of silver, iron oxide and Ag@Fe<sub>2</sub>O<sub>3</sub> CNPs.

**Keywords:** *Alstonia scholaris* leaf extract, Ag-Fe<sub>2</sub>O<sub>3</sub>CNPs, Ultrasound cavitation, Transmission electron microscopy, AgNPs, X-ray diffraction.

## 1. INTRODUCTION

The prospect of exploiting natural resources for metal nanoparticle synthesis has become a competent and environmentally benign approach [1]. Green synthesis of nanoparticles is an eco-friendly approach, which might pave the way for researchers across the globe to explore the potential of different herbs in order to synthesize nanoparticles [2]. Various researchers have reported synthesis of silver and gold nanoparticles using parts of herbal plants (bark of cinnamon, neem leaves, tannic acid and various plant leaves [3 - 7], fungi, honey, bacteria and yeast [8]. Nowadays development of eco-friendly procedures or green chemistry approach for the synthesis of nanomaterials is gaining fast momentum over the other methods of synthesis of nanomaterials. Green chemistry approach of nanomaterials synthesis

\* Address correspondence to this author at the Department of Chemistry, University of Mumbai, Sant Cruz (E) 400 098, India; E-mail: [navin\\_shimpi@rediffmail.com](mailto:navin_shimpi@rediffmail.com)

provides some valuable advantages such as cost effective, environment friendly, less time consuming, formation of minimal amount of byproducts and simplicity in scaling up for large scale synthesis where no considerable amounts of pressure, temperature, toxic chemicals, and energy is required.

In addition to metals and bimetallic nanoparticles, core-shell nanostructures are being increasingly investigated because of their wide applications and versatile nature [9 - 20]. Prasad *et al.* have obtained core-shell NPs using  $\text{Fe}(\text{acac})_3$  as the iron source and 1,2-alkanediol as the reducing agent [21]. Chen *et al.* have prepared Ag-  $\text{Fe}_2\text{O}_3$  hybrids nanoparticles using oleic acid and oleyl amine as surface-capping agents, and 1-dodecanol was used as both solvent and reducing agent [22]. However very few research is available on the synthesis of core shell nanoparticles using various plants extract. Rai *et al* studied and synthesize metal nanoparticles of Au-Ag CNPs having core of triangular geometry over the shell of Ag NPs using lemongrass extract [23].

*Alstonia scholaris* is available tremendously and is a native plant of Indian subcontinent, Indomalya, Malaysia and Australasia. In Indian subcontinent, the common name of *Alstonia scholaris* is Indian devil tree. *Alstonia scholaris* is member of apocynaceae family, which includes 46-60 species. Extract prepared from this plant containing some aldehyde and ketone compounds (alkaloids, flavonoids, pinocarvone and cryptone), which potentially could be used as a reducing and stabilizing agents.

The work deals with the in-situ synthesis of Ag- $\text{Fe}_2\text{O}_3$  CNPs using *Alstonia scholaris* leaf extract in aqueous medium under controlled ultrasound cavitation technique. So far core-shell synthesis using *Alstonia scholaris* leaf extract has not been yet reported elsewhere. Presence of active reducing and stabilizing agents in above leaf extract forms well stabilized metal and metal oxide nanoparticles with formation of core-shell nanoparticles. Previously this group has synthesized AgNPs using plant leaf extract and  $\text{Fe}_2\text{O}_3$  nanoparticles [24 - 26].

## 2. EXPERIMENTAL

### 2.1. Materials

The *Alstonia scholaris* plant leaves were collected from surrounding of hilly region of Khandesh (Maharashtra, India). Other chemicals required for the synthesis of silver nanoparticles and core-shell nanoparticles such as silver nitrate, iron nitrate were procured from Merck, India.

### 2.2. Preparation of the Leaf Extracts Using Ultrasonic Cavitation Technique

The collected samples were brought to the laboratory and washed using fresh water to remove the contaminants from the leaf surface (Fig. 1), which were shade dried for 15 days under dust free condition. These dried leaves were cut into small pieces and grounded into fine powder on grinder. This powder was sieved using 75  $\mu\text{m}$  mesh size sieve shaker. The extract was prepared using this powder (25 gm) in millipore water (100 ml). This mixture was sonicated for 40 min (B03-Ultrasonic Processor make E-Chrom Tech., Taiwan) at pulse rate of 5 sec on and off with intensity 20 KHz. The color of the solution turns to a light yellow (Fig. 2). This leaf extract was allowed to cool at room temperature and filtered using Whatmann filter paper No.1. This extract was stored in refrigerator to protect it from fungal growth. Further this extract was used as reducing and capping or stabilizing agent for the synthesis of AgNPs,  $\alpha\text{-Fe}_2\text{O}_3$ NPs and Ag- $\text{Fe}_2\text{O}_3$  CNPs.



**Fig. (1).** *Alstonia scholaris* plant leaves.

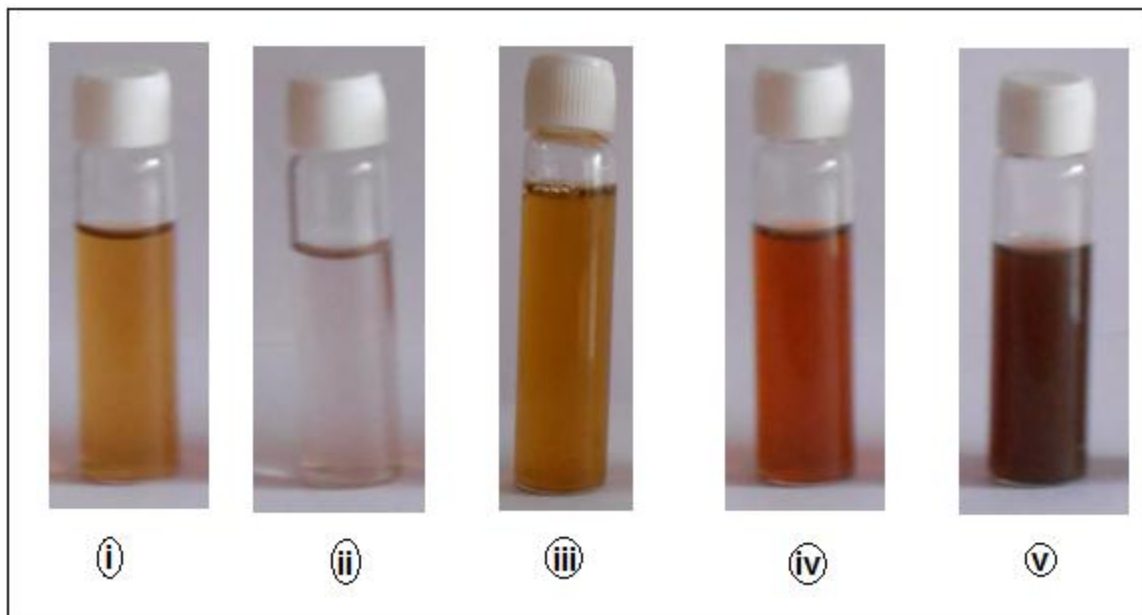


**Fig. (2).** Solutions of i) *Alstonia scholaris* plant leaf extract, ii) silver nitrate solution, iii) iron nitrate solution, iv) Colloidal suspension of AgNPs, v) Colloidal suspension of Ag-Fe<sub>2</sub>O<sub>3</sub>CNPs.

### 2.3. Synthesis of Ag NPs and $\alpha$ -Fe<sub>2</sub>O<sub>3</sub> NPs

0.01 M silver nitrate (AgNO<sub>3</sub>) was added drop wise into *Alstonia scholaris* leaf extract (25 ml) under controlled ultrasound assisted cavitation technique. The pulse rate was maintained at 5 sec on/off till the complete addition. The mixture was sonicated for additional one hour at same pulse rate and intensity (20 KHz). During this process, the color of colloidal suspension was change from yellowish to light brown. Further the particles were isolated from this colloidal suspension using ethanol as a non-solvent. The Ag particles were dried in hot air oven at 80 °C for one hour. Similar procedure was adopted for the synthesis of  $\alpha$ -Fe<sub>2</sub>O<sub>3</sub> NPs using 0.01 M iron nitrate.

### 2.3. Synthesis of Ag-Fe<sub>2</sub>O<sub>3</sub>CNPs

The Ag-Fe<sub>2</sub>O<sub>3</sub>CNPs were prepared by taking colloidal suspension of AgNPs (25 ml) to which the colloidal solution of  $\alpha$ -Fe<sub>2</sub>O<sub>3</sub>NPs were added drop wise under controlled ultrasound cavitation technique. The pulse rate was 5 sec on/off throughout the reaction at intensity 20 KHz. The color of colloidal suspension was appears to be dark during the process. After complete sonication, the particles were isolated from colloidal suspension using ethanol as a non-solvent. Ag-Fe<sub>2</sub>O<sub>3</sub>CNPs particles were dried in hot air oven at 80 °C for one hour. The core was of AgNPs, while the shell of  $\alpha$ -Fe<sub>2</sub>O<sub>3</sub>NPs.

## 3. CHARACTERIZATIONS

### 3.1. UV-visible Spectroscopy (UV)

UV-Vis absorption spectra at resolution of 2 nm were recorded on a double beam spectrophotometer 1800 (Shimadzu, Tokyo, Japan) in a wavelength range between 300-600 nm.

### 3.2. X-ray Diffraction (XRD)

X-ray diffraction (XRD) analysis was conducted to know about the size of particles on Brukers D8 advance X-ray diffractometer (Germany) with CuK $\alpha$ , radiation ( $\lambda=1.5404$  Å) at 30 kV & 40 mA at scanning range of 10-80° with intensity 2500 cps.

### 3.3. Transmission Electron Microscopy (TEM)

A transmission electron microscope (TEM) (Philips CM200, Netherlands) was used to assess the morphology and size of nanomaterials at a resolution of 2.4 Å. The samples were dispersed in ethanol and deposited on a copper grid

before viewing under the microscope.

### 3.4. Field Emission-Scanning Electron Microscopy (FE-SEM) and Energy Dispersive X-ray Spectroscopy (EDAX)

The FE-SEM analysis was done on field emission-scanning electron microscopy (FE-SEM) (Hitachi S-4800, Tokyo, Japan) used to assess the surface morphology and energy dispersive X-ray spectroscopy (EDAX) for the elemental analysis. The samples were dispersed in ethanol and mounted on specimen tub with a gold coating before viewing under the microscope.

### 3.5. Fourier Transform Infrared (FTIR) Spectroscopy

A Fourier transform infrared (FTIR) spectrum was recorded on FTIR-8400 spectrophotometer (Shimadzu, Tokyo, Japan) within the spectral range of 500 - 4000  $\text{cm}^{-1}$  with a resolution of 4  $\text{cm}^{-1}$ . The samples were prepared in the pellet form by mixing potassium bromide (KBr) as a binder.

## 4. RESULTS AND DISCUSSION

### 4.1. Mechanism of Nanoparticles Formation by Ultrasound Induced Cavitation

Fig. (3) shows a schematic presentation of AgNPs,  $\alpha\text{-Fe}_2\text{O}_3$ NPs and Ag- $\text{Fe}_2\text{O}_3$ CNPs. Ultrasound assisted synthesis involves the cavitation mechanism, which refers to the formation, growth and collapse of bubbles due to transmission of acoustic waves through a medium which ruptures the molecular structure of the medium (Fig. 3). During cavitation, bubbles grow due to the diffusion of  $\text{Ag}^+$  into it by implosive collapse and get concentrated at the interface where they react with the high energy species and along with beginning of nucleation. The formed nanoparticles are bounded by the layer(s) of various stabilizing agents, which are present in plant extract, which protects the particles from agglomeration arise due to strong charges over the surface of ions such as Ag and Fe ions. On reaching its maximum size, the bubble undergoes implosive collapse, which resulting high temperature of the solution attaining along with faster cooling rate. At such fast kinetics the growth of the nuclei is hindered and consequently, nanosized silver particles are formed and reduction takes place. These nanoparticles have a large number of dangling bonds on their surface. For surface stability bond formation is necessary, which leads to growth of nuclei. But when the growth is stopped prematurely, the stabilization of the silver nanoparticles occur through bond formation with stabilizing agents present in the plant extract of *Alstonia scholaris* which prevents aggregation of nanoparticles (Fig. 6a). Further the formation of CNPs using Ag and iron oxide was continued by in-situ method under ultrasound cavitation technique. The shell formation was took place over the core of AgNPs. The core and shell bonding is took place due to presence of bonding agent in *Alstonia scholaris* leaf extract.

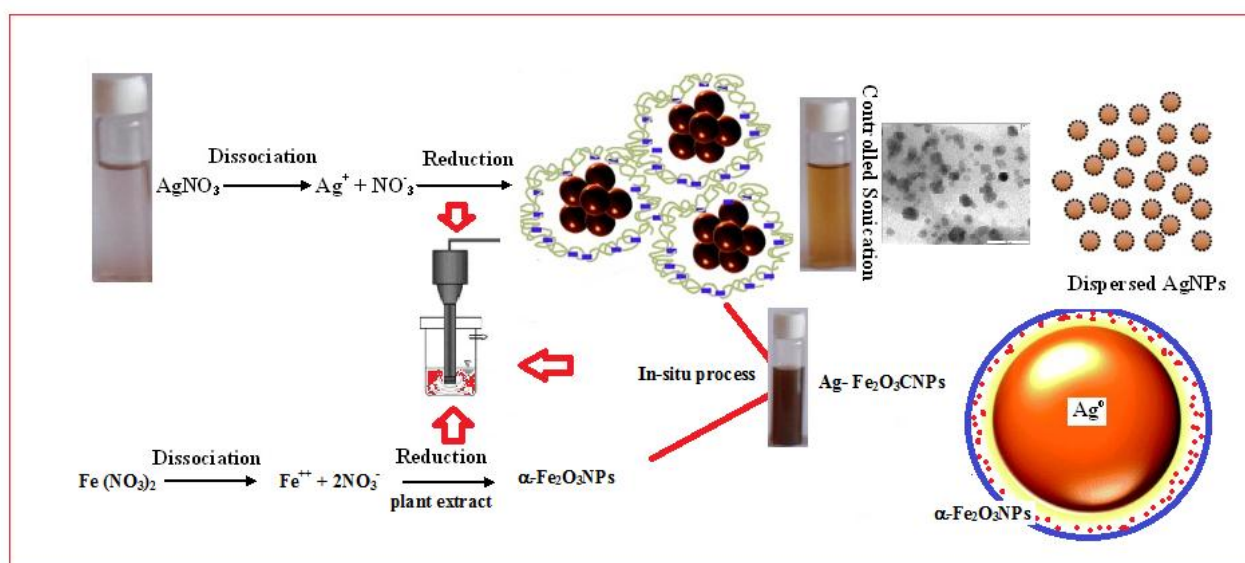


Fig. (3). Mechanism of AgNPs,  $\alpha\text{-Fe}_2\text{O}_3$ NPs and Ag- $\text{Fe}_2\text{O}_3$ CNPs formation.

#### 4.2. UV-Visible Spectroscopy (UV)

AgNPs and Ag-Fe<sub>2</sub>O<sub>3</sub>CNPs formation by *Alstonia scholaris* leaf extract of green synthesis approach was studied using UV-Vis spectroscopy. The sharp peak at visible region is evidence for the formation of AgNPs and Ag-Fe<sub>2</sub>O<sub>3</sub>CNPs. Metal and core-shell particles (AgNPs and Ag-Fe<sub>2</sub>O<sub>3</sub>CNPs) possess free electrons abundantly, which moves through conduction and valence band. These free electrons are responsible for surface plasmon resonance (SPR) absorption band and broad peak with red shift from the core for core-shell particles. It was observed that AgNPs exhibits surface plasmon resonance (SPR) absorption at 375 nm, while Ag-Fe<sub>2</sub>O<sub>3</sub>CNPs shows broad peak with a red shift from the core of AgNPs (Figs. 4a, b). The large shift of the SPR peak can be accounted by the local dielectric effect, as the oxide shell has higher refractive index of 2.4, which turns to red-shift from SPR absorption band according to classical Mie theory. A similar phenomenon has been observed elsewhere [27].

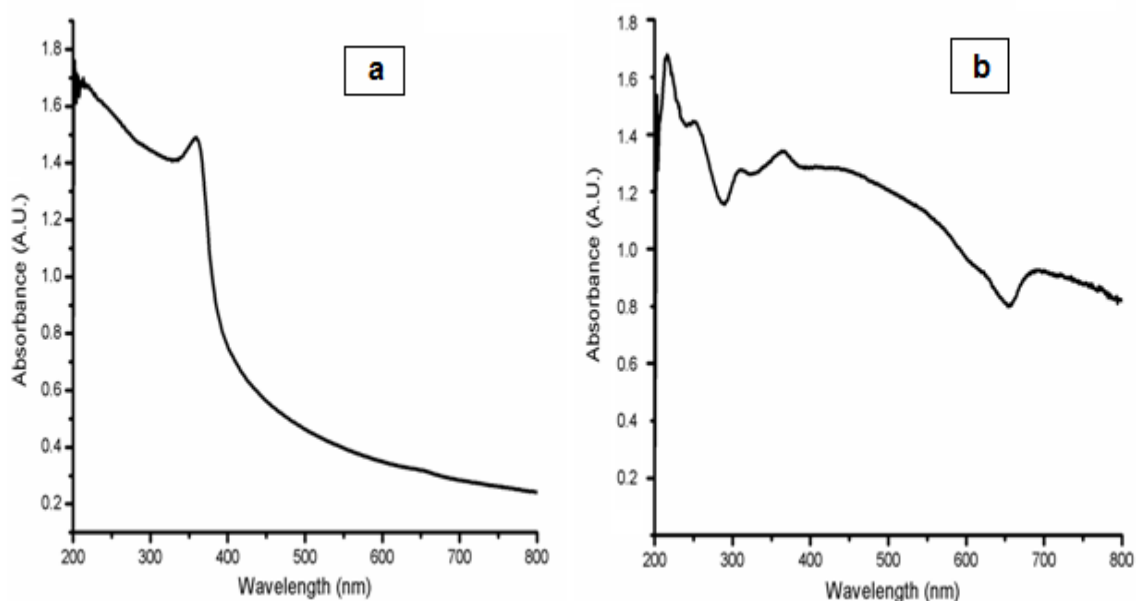


Fig. (4). UV-Vis of AgNPs and Ag- Fe<sub>2</sub>O<sub>3</sub>CNPs.

#### 4.3. X-Ray Diffraction (XRD)

The crystallite domain size was calculated from the width of the XRD peaks, assuming that they are free from non-uniform strains, using the following Scherer's formula.

$$D = 0.94 \lambda / \beta \cos \theta \quad (1)$$

Where, D is the average crystallite domain size perpendicular to the reflecting planes,  $\lambda$  is the X-ray wavelength,  $\beta$  is the full width at half maximum (FWHM), and  $\theta$  is the diffraction angle. (Fig. 5) shows the XRD pattern of Ag-Fe<sub>2</sub>O<sub>3</sub>CNPs, AgNPs and  $\alpha$ -Fe<sub>2</sub>O<sub>3</sub>NPs. The peak at 24°, 31°, 39°, 43°, 65°, 67° and 75° corresponds to crystal planes (012), (104), (111), (200), (220), (300) and (311). The sets of crystal plane such (012), (104), (116) and (300) other the crystal planes of AgNPs and  $\alpha$ -Fe<sub>2</sub>O<sub>3</sub>NPs indicates the formation of core-shell. The peaks at 39°, 43°, 65° and 75° corresponds to (111), (200), (220) and (311) planes. These planes can be indexed as face-centered -cubic structure (FCC) of AgNPs, whereas crystal planes at (111), (200), (220), (311), (400), (422) and (511) for  $\alpha$ - Fe<sub>2</sub>O<sub>3</sub>NPs. There is no any additional peak, which is the indication of formation of high purity product. This effective formation of Ag-Fe<sub>2</sub>O<sub>3</sub>CNPs AgNPs and  $\alpha$ - Fe<sub>2</sub>O<sub>3</sub>NPs was due to synthesis using *Alstonia scholaris* leaf extract, which doesn't form any side products.

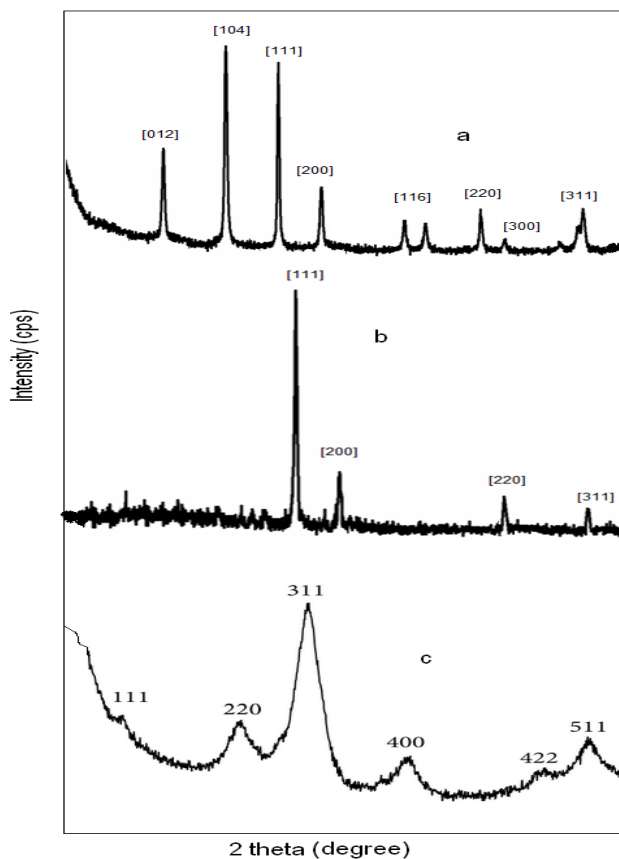


**Fig. (5).** (a) Ag-Fe<sub>2</sub>O<sub>3</sub>CNPs (b) AgNPs (c) α-Fe<sub>2</sub>O<sub>3</sub>NPs.

#### 4.4. Transmission Electron Microscopy (TEM)

The morphology of Ag-αFe<sub>2</sub>O<sub>3</sub>CNPs and AgNPs was studied using transmission electron microscopy. It was observed that AgNPs having spherical as well as triangular pyramidal shape with minimal aggregated structures. The size of AgNPs was found to be ~15-38 nm. Figs. (6a, b) shows the TEM of Ag-αFe<sub>2</sub>O<sub>3</sub>CNPs. It was found that the core (AgNPs) having dark black shade, while the shell (αFe<sub>2</sub>O<sub>3</sub>NPs) is having faint grey shade. The overall diameter of Ag-αFe<sub>2</sub>O<sub>3</sub>CNPs was ≈50 nm, while diameter of AgNPs core was ≈10 nm with αFe<sub>2</sub>O<sub>3</sub>NPs thickness over core is ≈4 nm. Fig. (6c) in inset clearly shows the Ag-αFe<sub>2</sub>O<sub>3</sub>CNPs. Fig. (6c) shows the clear view of core-shell nanoparticles.

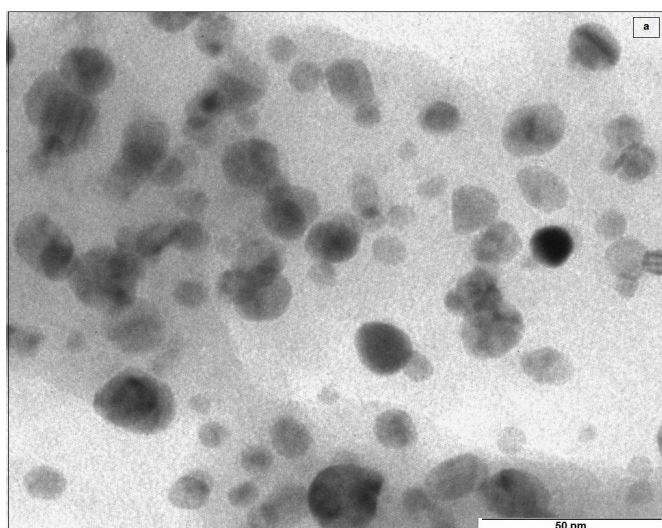


**Fig. (6a).** TEM of AgNPs.

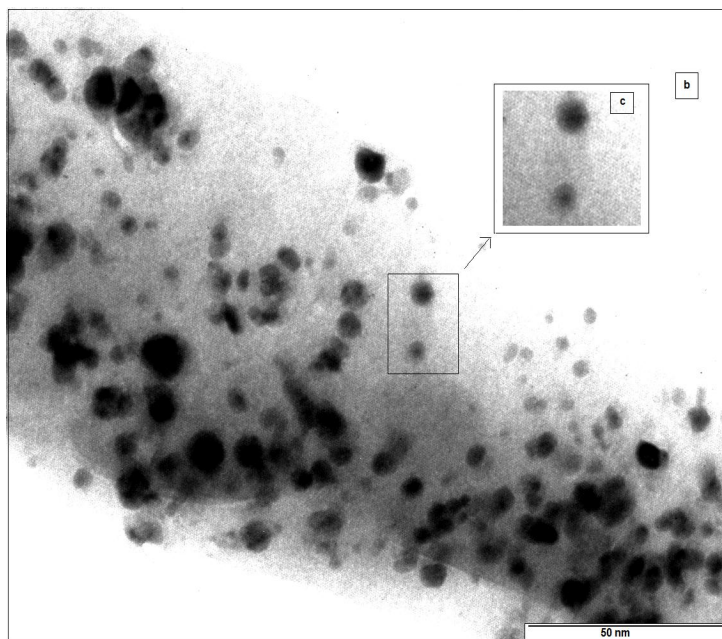


**Fig. (6b).** TEM of Ag-  $\text{Fe}_2\text{O}_3$  CNPs (c) Inset of core-shell structure.

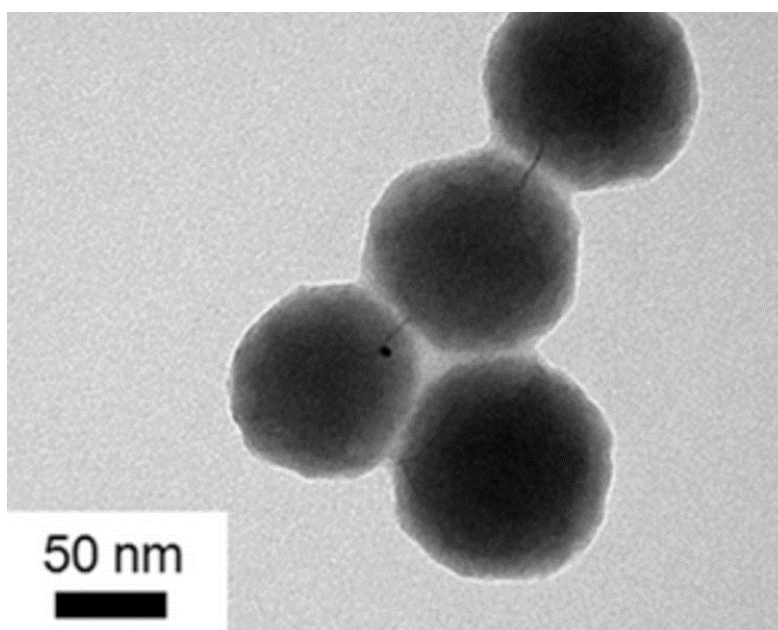


**Fig. (6c).** TEM of Ag-  $\text{Fe}_2\text{O}_3$  CNPs (Clear image).

#### 4.5. Field Emission-Scanning electron microscopy (FE-SEM) and Energy Dispersive X-ray Spectroscopy (EDAX)

Fig. (7a-b) shows FE-SEM of AgNPs & Ag- $\alpha\text{Fe}_2\text{O}_3$  CNPs synthesized using *Alstonia scholaris* leaf extract. It can be observed that most of AgNPs were of spherical shape having size  $\sim 17\text{-}51$  nm, while Ag- $\alpha\text{Fe}_2\text{O}_3$  CNPs having diameter  $\approx 50$  nm with core of AgNPs and shell of  $\alpha\text{Fe}_2\text{O}_3$  NPs. The particle size and shape as seen in FESEM is in line with TEM. Moreover, Figs. (8a, b) shows the energy-dispersive X-ray spectroscopy (EDAX) for AgNPs & Ag- $\alpha\text{Fe}_2\text{O}_3$  CNPs synthesized using *Alstonia scholaris* leaf extract to examine the composition and purity. Elemental silver could be seen in the graph presented by the EDAX analysis, which indicates the reduction of silver ions to elemental silver by *Alstonia scholaris* leaf extract. Moreover the presence of elemental silver ion along with the iron oxide indicates the formation of Ag- $\alpha\text{Fe}_2\text{O}_3$  CNPs. The vertical axis displays the number of X-ray counts while the horizontal axis displays energy in keV.

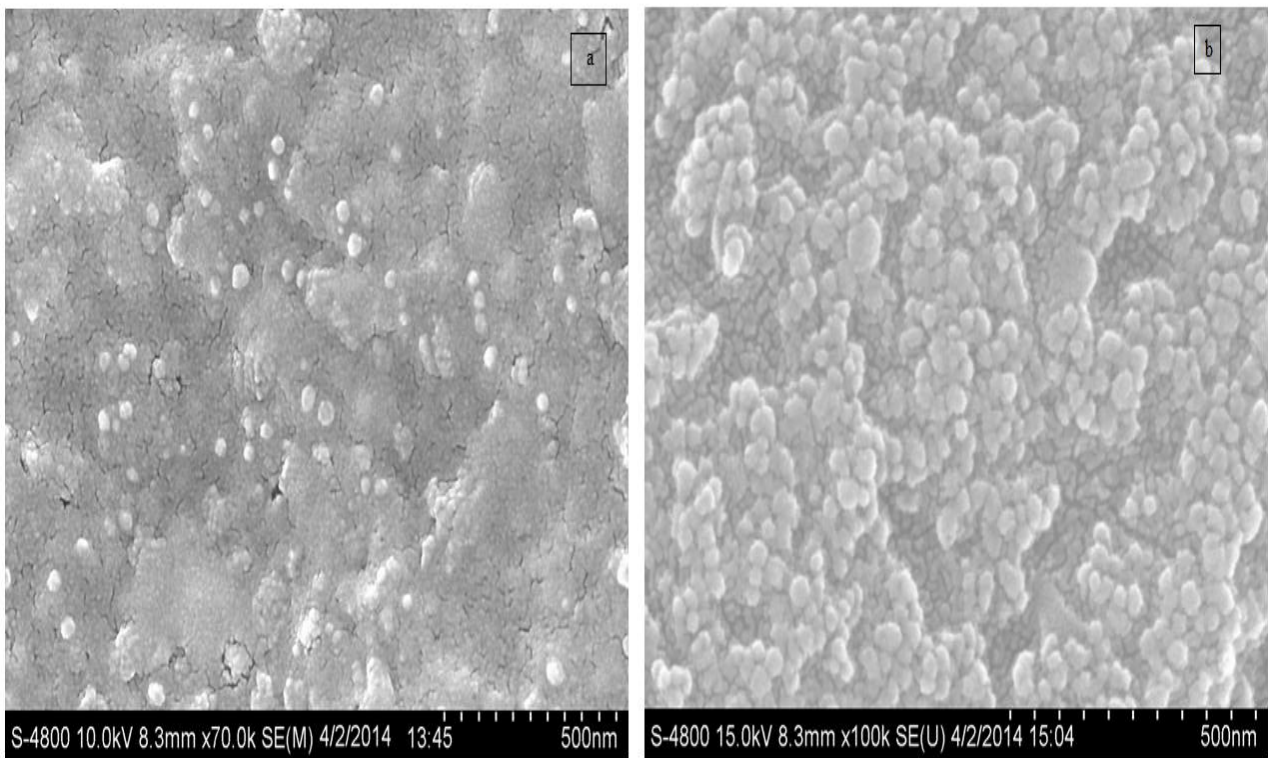


Fig. (7). FESEM AgNPs and Ag- Fe<sub>2</sub>O<sub>3</sub>CNPs.

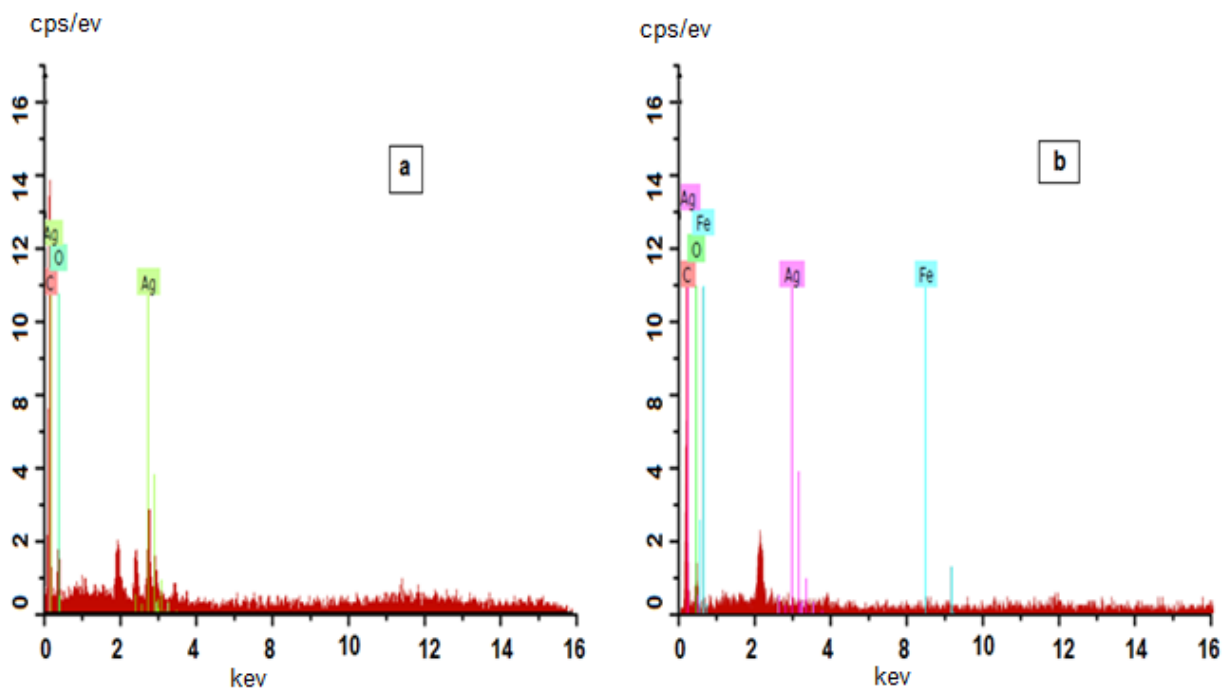


Fig. (8). EDAX of AgNPs and Ag- Fe<sub>2</sub>O<sub>3</sub>CNPs.

#### 4.6. Fourier Transform Infrared (FT-IR) Spectroscopy

FT-IR spectroscopy was applied to identify the potential functional groups presented in the bio molecules of *Alstonia scholaris* leaf extract, which are responsible for reducing the silver ions as well as formation of core-shell

nanoparticles. A representative FTIR spectrum of the synthesized AgNPs, Ag- $\alpha$ -Fe<sub>2</sub>O<sub>3</sub>CNPs &  $\alpha$ -Fe<sub>2</sub>O<sub>3</sub>NPs was shown in Figs. (9a-c). The peaks at 3400, 1568, 1492, 1383, 903, 510 cm<sup>-1</sup> in the region of 500-3400 cm<sup>-1</sup> was the indication of formation of AgNPs using *Alstonia scholaris* leaf extract as reducing agent Fig. (9a). The indicative absorption peak at 3364 cm<sup>-1</sup> attributed to N-H stretching for primary and secondary amine or amide functional groups. Besides this the peak at 1568-1492 cm<sup>-1</sup> might be due to asymmetric stretching vibrations of -N-O and peak at 1383 cm<sup>-1</sup> was for symmetric stretching vibration of -N-O functional group. The absorption peaks 903 cm<sup>-1</sup> can be assigned as the absorption peaks of -C-N waging of primary or secondary amines and peak at 510 cm<sup>-1</sup> can be attributed due to C-X stretch of alkyl halide (X is any halide group) [28]. Fig. (9b) shows the FT-IR of Ag- $\alpha$ -Fe<sub>2</sub>O<sub>3</sub>CNPs. Number peaks were observed and the major indicative peaks are 3400, 1532, 1442, 1072, 550 cm<sup>-1</sup> in the region of 500-3400 cm<sup>-1</sup>. Moreover the same phenomenal observation was in case of  $\alpha$ -Fe<sub>2</sub>O<sub>3</sub>NPs Fig. (9c). The indicative absorption peak at 3380 cm<sup>-1</sup> attributed to N-H stretching for primary and secondary amine or amide functional groups.

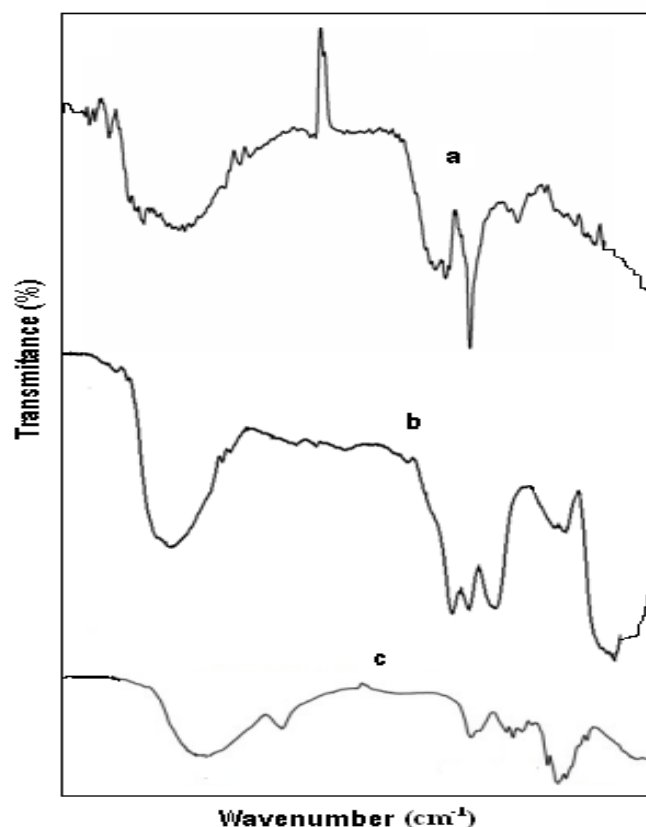


Fig. (9). FTIR of (a) AgNPs (b) Ag- Fe<sub>2</sub>O<sub>3</sub>CNPs (c)  $\alpha$ -Fe<sub>2</sub>O<sub>3</sub>NPs.

## CONCLUSION

In essence, *Alstonia scholaris* leaf extract prepared in aqueous medium was used to synthesis AgNPs,  $\alpha$ -Fe<sub>2</sub>O<sub>3</sub>NPs and Ag- Fe<sub>2</sub>O<sub>3</sub>CNPs. Presence of aldehydic and ketonic functional compounds acts as a reducing agent for Ag<sup>+</sup> and Fe<sup>+2/+3</sup> ions. Whereas few waxy compounds available in plant extract may acts as a capping and/or stabilizing agent, which makes the core-shell nanomaterials very stable and effective. This method of synthesis of core-shell nanoparticles was found to be facile and a complete green chemistry approach due to use of *Alstonia scholaris* leaf extract which is prepared under aqueous medium. The size of AgNPs and  $\alpha$ -Fe<sub>2</sub>O<sub>3</sub>NPs was found to be ~15-38 nm and ~25-45 nm, respectively. The controlled particles size and diameter of core-shell was found to be very effective due to active reducing agents as well as stabilizing agents present in *Alstonia scholaris* leaf extract and also due to effective dispersion of ions through the solution using ultrasound cavitation technique. During cavitation, bubbles grow due to the diffusion of ions into it by implosive collapse and get concentrated at the interface where they react with the high energy species and nucleation begins. But as soon as the particles are formed they are bound by the layer(s) of various stabilizing agents present in plant extract through electrostatic forces of *Alstonia scholaris* extract. On reaching its

maximum size the bubble undergoes implosive collapse resulting in the solution attaining very high temperature (up to about 24,000 K) along with very high cooling rate.

#### CONSENT FOR PUBLICATION

Not applicable.

#### CONFLICT OF INTEREST

The authors declare no conflict of interest, financial or otherwise.

#### ACKNOWLEDGEMENTS

Authors are thankful to UGC, New Delhi for providing financial assistance to carry out this work under UGC major research project [UGC/MRP/43-157/2014 (SR)].

#### REFERENCES

- [1] Bhattacharya D, Gupta RK. Nanotechnology and potential of microorganisms. *Crit Rev Biotechnol* 2005; 25(4): 199-204. [<http://dx.doi.org/10.1080/07388550500361994>] [PMID: 16419617]
- [2] Savithramma N, Rao ML, Devi PS. *J Biol Sci* 2011; 11: 39. [<http://dx.doi.org/10.3923/jbs.2011.39.45>]
- [3] Sathishkumar M, Sneha K, Won SW, Cho CW, Kim S, Yun YS. Cinnamon zeylanicum bark extract and powder mediated green synthesis of nano-crystalline silver particles and its bactericidal activity. *Colloids Surf B Biointerfaces* 2009; 73(2): 332-8. [<http://dx.doi.org/10.1016/j.colsurfb.2009.06.005>] [PMID: 19576733]
- [4] Tripathi A, Chandrasekaran N, Raichur AM, Mukherjee AJ. *Biomed Nanotechnol* 2009; 5: 93. [<http://dx.doi.org/10.1166/jbn.2009.038>]
- [5] Prathna TC, Chandrasekaran N, Raichur AM, Mukherjee A. Biomimetic synthesis of silver nanoparticles by Citrus limon (lemon) aqueous extract and theoretical prediction of particle size. *Colloids Surf B Biointerfaces* 2011; 82(1): 152-9. [<http://dx.doi.org/10.1016/j.colsurfb.2010.08.036>] [PMID: 20833002]
- [6] Sivaraman SK, Elango I, Kumar S, Santhanam V. *Curr Sci* 2009; 97: 1055.
- [7] Song JY, Kim BS. Rapid biological synthesis of silver nanoparticles using plant leaf extracts. *Bioprocess Biosyst Eng* 2009; 32(1): 79-84. [<http://dx.doi.org/10.1007/s00449-008-0224-6>] [PMID: 18438688]
- [8] Begum N A, Mondal S, Basu S, Laskara R A. *Colloid Surf. B* 2009, 113-118
- [9] Nair S, Tom RT, Rajeev Kumar VR. *C Subramaniam And T Pradeep Cosmos* 2007; 3: 103-24. [<http://dx.doi.org/10.1142/S0219607707000244>]
- [10] Yang J, Yang Lee J, Deivaraj T C. *Colloids Surf A Physicochem Eng Asp* 2014; 240: 131-4. [<http://dx.doi.org/10.1016/j.colsurfa.2004.03.019>]
- [11] Sun S, Murray CB, Weller D, Folks L, Moser A. Monodisperse FePt nanoparticles and ferromagnetic FePt nanocrystal superlattices. *Science* 2000; 287(5460): 1989-92. [<http://dx.doi.org/10.1126/science.287.5460.1989>] [PMID: 10720318]
- [12] Pelton M, Aizpurua J, *Rev G B. Rev.* 2,3, (2008) 136 [<http://dx.doi.org/10.1002/lpor.200810003>]
- [13] McConnell WP, Novak JP, Brousseau LC III, Fuierer RR, Tenent RC, Feldheim DL. *J Phys Chem B* 2000; 104: 8925. [<http://dx.doi.org/10.1021/jp000926t>]
- [14] Chen S. Y. *ang. J Am Chem Soc* 2002; 124: 5280. [<http://dx.doi.org/10.1021/ja025897+>] [PMID: 11996564]
- [15] Han SW, Kim Y, Kim K. Dodecanethiol-Derivatized Au/Ag Bimetallic Nanoparticles: TEM, UV/VIS, XPS, and FTIR analysis. *J Colloid Interface Sci* 1998; 208(1): 272-8. [<http://dx.doi.org/10.1006/jcis.1998.5812>] [PMID: 9820774]
- [16] Link S, Wang ZL, El-Sayed MA. *J Phys Chem B* 1999; 103: 3529. [<http://dx.doi.org/10.1021/jp990387w>]
- [17] Jiang W, Zhou Y, Zhang Y, Xuan S, Gong X. Superparamagnetic Ag@Fe<sub>3</sub>O<sub>4</sub> core-shell nanospheres: Fabrication, characterization and application as reusable nanocatalysts. *Dalton Trans* 2012; 41(15): 4594-601. [<http://dx.doi.org/10.1039/c2dt12307j>] [PMID: 22354183]
- [18] Caruso F. *Adv Mater* 2001; 13: 11. [[http://dx.doi.org/10.1002/1521-4095\(200101\)13:1<11::AID-ADMA11>3.0.CO;2-N](http://dx.doi.org/10.1002/1521-4095(200101)13:1<11::AID-ADMA11>3.0.CO;2-N)]

- [19] Schmid G. Chem Rev 1992; 92: 1709.  
[<http://dx.doi.org/10.1021/cr00016a002>]
- [20] Aiken JD III, Finke RG. J Mol Catal A 1999; 145: 1.  
[[http://dx.doi.org/10.1016/S1381-1169\(99\)00098-9](http://dx.doi.org/10.1016/S1381-1169(99)00098-9)]
- [21] Shi W, Zeng H, Sahoo Y, *et al.* Nano Lett 2006; 6: 875.  
[PMID: 16608302]
- [22] Chen Y, Gao N, Jiang J. Surface matters: enhanced bactericidal property of core-shell Ag-Fe<sub>2</sub>O<sub>3</sub> nanostructures to their heteromer counterparts from one-pot synthesis. Small 2013; 9(19): 3242-6.  
[PMID: 23585383]
- [23] Rai A, Chaudhary M, Ahmad A, Bhargava S, Sastry M. Mater Res Bull 2007; 42: 1212.  
[<http://dx.doi.org/10.1016/j.materresbull.2006.10.019>]
- [24] Navinchandra G Shimpi, Minakshi Jha. Green synthesis of zero valent colloidal nanosilver targeting A549 lung cancer cell: *In vitro* cytotoxicity. Journal of Genetic Engineering and Biotechnology  
[<http://dx.doi.org/10.1016/j.jgeb.2017.12.001>]
- [25] Navinchandra G Shimpi, Minakshi Jha. IJPSR. 2017; 8: pp. (12)5100-10.
- [26] T. Sen, N. G. Shimpi, S. Mishra, R. Sharma. Polyaniline/Gama Fe2O3 Nanocomposites for room temperatures, Sensors and Actuators B: chemical. 2014; 190: pp. 120-6.
- [27] Shi W, Zeng H, Sahoo Y, *et al.* A general approach to binary and ternary hybrid nanocrystals. Nano Lett 2006; 6(4): 875-81.  
[<http://dx.doi.org/10.1021/nl0600833>] [PMID: 16608302]
- [28] Luo L-B, Yu S-H, Qian H-S, Zhou T. Large-scale fabrication of flexible silver/cross-linked poly(vinyl alcohol) coaxial nanocables by a facile solution approach. J Am Chem Soc 2005; 127(9): 2822-3.  
[<http://dx.doi.org/10.1021/ja0428154>] [PMID: 15740096]

---

© 2018 Shimpi *et al.*

This is an open access article distributed under the terms of the Creative Commons Attribution 4.0 International Public License (CC-BY 4.0), a copy of which is available at: <https://creativecommons.org/licenses/by/4.0/legalcode>. This license permits unrestricted use, distribution, and reproduction in any medium, provided the original author and source are credited.